



Supplement of

The global aerosol–climate model ECHAM6.3–HAM2.3 – Part 2: Cloud evaluation, aerosol radiative forcing, and climate sensitivity

David Neubauer et al.

Correspondence to: David Neubauer (david.neubauer@env.ethz.ch)

The copyright of individual parts of the supplement might differ from the CC BY 4.0 License.

1 L47 vs. L31 and E63H23-GFAS34 and E63H23-10CC

The simulation of E63H23 with 31 vertical levels (L31) instead of 47 vertical levels (L47) show similar results to L47 (the additional levels are added mostly in the stratosphere; model top increases from 10 hPa to 0.01 hPa). Table S1 shows the results of the simulations E63H23-L31, E63H23-GFAS34 and E63H23-10CC which can be compared to the values of
5 E63H23 in Table 2. Also the values for the time period 2000-2009 are shown for E63H23, which are quite similar to those of the time period 2003-2012 in Table 2. Therefore the values of the different model versions in Table 2 can be compared although they cover slightly different time periods. As an example for the similar results for L31 and L47 in E63H23, Figure S1 shows the global mean IWC as a function of pressure for E63H23 and the two vertical grids, L31 and L47. The IWC lines of both vertical grids lie almost on top of each other.

Table S1. Global mean values of the PD simulations for E63H23 but for the period 2000-2009, E63H23-L31, E63H23-GFAS34, E63H23-10CC, E63H23-LL and E63H23-GUELLE. Radiative fluxes are at the top of atmosphere. Values from observations (OBS) and multi-model means (MMM) are shown next to those of the three model versions. $\text{ERF}_{\text{ari+aci}}$ and ECS are from the $\text{PD}_{\text{aer}}/\text{PI}_{\text{aer}}$ and $1\times\text{CO}_2/2\times\text{CO}_2$ simulations respectively.

5

Variable	OBS/MMM	E63H23 (2000- 2009)	E63H23- L31 (2003- 2012)	E63H23- GFAS34 (2003- 2012)	E63H23- 10CC (2003- 2012)	E63H23- LL (2003- 2012)	E63H23- GUELLE (2003- 2012)
SW (W m^{-2})	240 (238 to 244)	238	238	238	238	240	239
LW (W m^{-2})	-239 (-237 to -241)	-238	-238	-238	-238	-238	-238
Net(W m^{-2})	0.7±0.1	0.4	0.5	0.0	0.5	1.5	1.6
SW CRE (W m^{-2})	-47 (-46 to 53.3)	-50	-50	-50	-50	-49	-48
LW CRE (W m^{-2})	26 (22 to 30.5)	24	24	24	24	24	24
Net CRE (W m^{-2})	-21 (-17.1 to 22.8)	-26	-26	-26	-25	-25	-24
CC (%)	68±5	69	68	68	69	68	68
LWP (ocean) (g m^{-2})	42.9 to 89.4	71	71	72	90	65	65
LWP-LP (ocean) (g m^{-2})	73.5±5.5	77	77	79	101	72	69
IWP (g m^{-2})	25±7	15	15	15	15	15	15
Cloud-top CDNC (ocean; 60°N-60°S) (cm^{-3})	72±37	78	78	84	73	70	67
CDNC _{burden} (10^{10} m^{-2})	-	3.1	3.1	3.3	2.9	2.6	2.7
ICNC _{burden} (10^{12} m^{-2})	-	8.0	8.0	7.8	8.1	7.9	7.9
P (mm d^{-1})	2.7±0.2	3.0	3.0	3.0	3.0	3.0	3.0
Sulfate burden (Tg)	2.0(±25%)	2.2	2.3	2.4	2.4	2.2	2.2
Black carbon burden (Tg)	0.2(±42%)	0.1	0.1	0.3	0.1	0.1	0.1
Particulate organic matter burden (Tg)	1.7(±27%)	1.0	1.0	2.2	1.1	1.0	1.0
Sea salt burden (Tg)	7.5(±54%)	4.1	4.1	4.1	4.3	4.0	10.2
Mineral dust burden (Tg)	19.2(±40%)	17.7	18.3	18.3	20.1	19.3	18.5
$\text{ERF}_{\text{ari+aci}}$ (W m^{-2})	-0.9 (-1.9 to -0.1)	-1.0	-1.0	-0.9	-1.7	-0.9	-0.9
ECS (K)	1.5 to 4.5	2.5	2.5	2.6	2.8	-	-

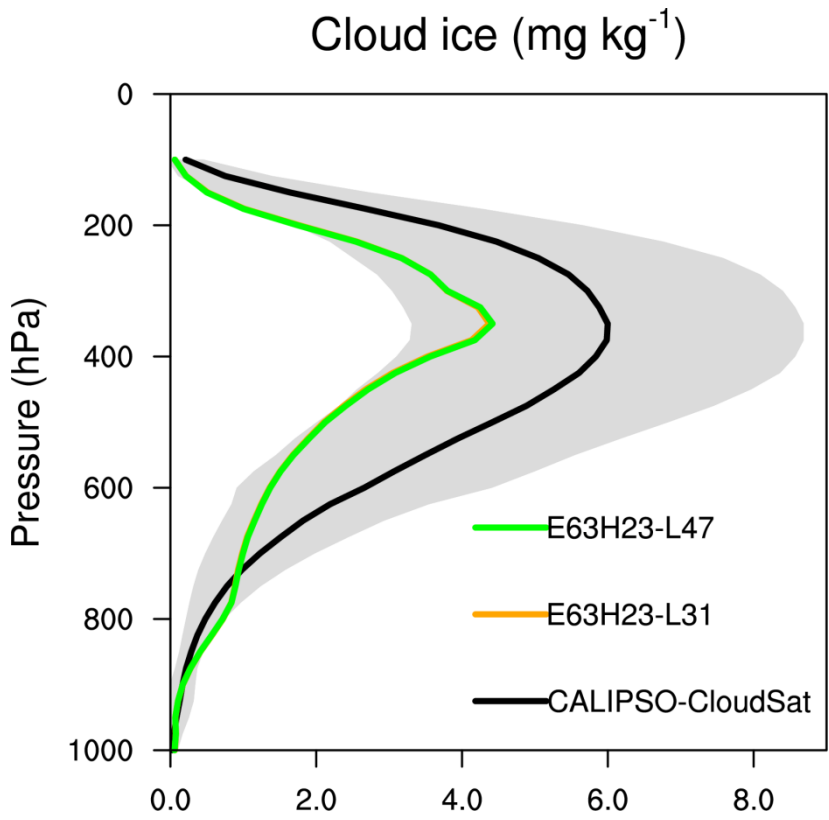


Figure S1: Comparison of global annual mean IWC as a function of pressure of E63H23 for the vertical grids L31 and L47 (default) to CALIPSO/CloudSat observations from Li et al. (2012). Gray shading indicates the uncertainty in the CALIPSO/CloudSat observations. The CALIPSO/CloudSat data covers the years 2006-2010, model data is from the PD simulations.

5

2 Frequency of convection

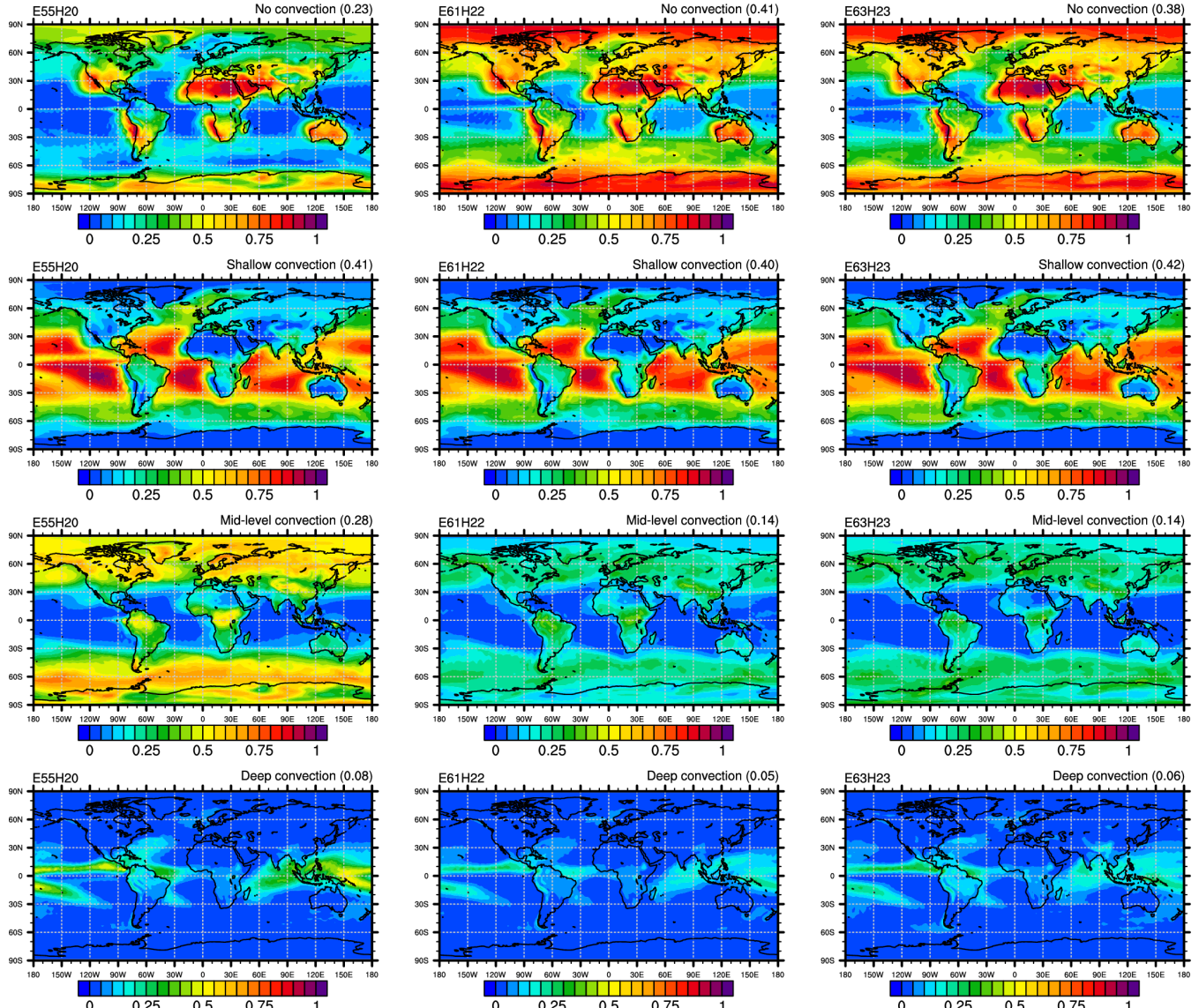


Figure S2: Annual mean frequency of the activation of the convection scheme for the different types of convection in E55H20, E61H22 and E63H23 PD simulations. Global annual mean values are shown in brackets.

3 ERF_{ari+aci}: Representative years; land vs. ocean and E63H23-GFAS34 and E63H23-10CC

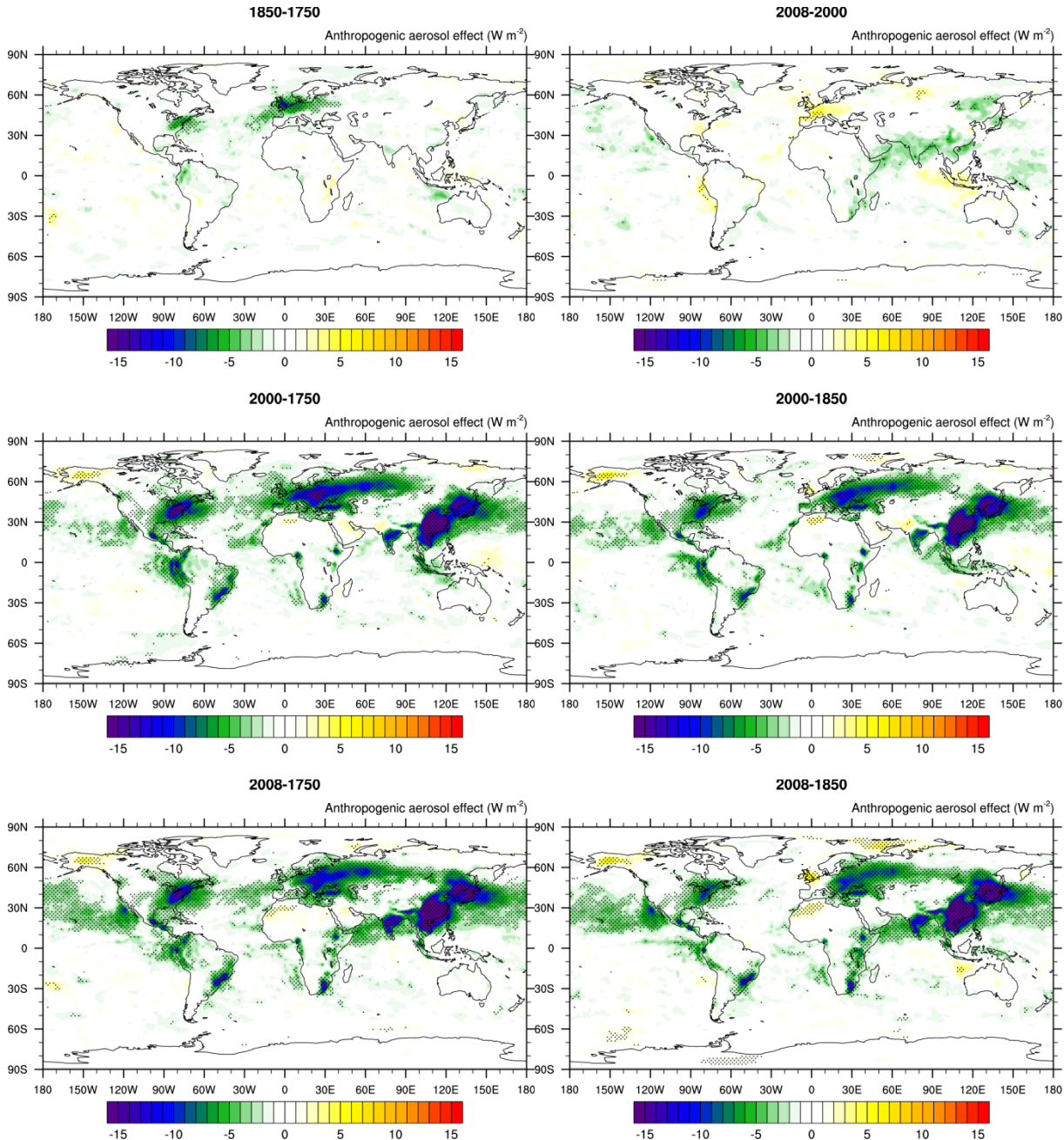


Figure S3: Global maps of Net ERF_{ari+aci} of E63H23 from 20 year free simulations with present day minus pre-industrial aerosol emissions (PD_{aer}-PI_{aer}). Different years are used to represent present day and pre-industrial aerosol emissions. Hatching indicates statistically significant differences at the 95% significance level. The false discovery rate is controlled following Wilks (2016).

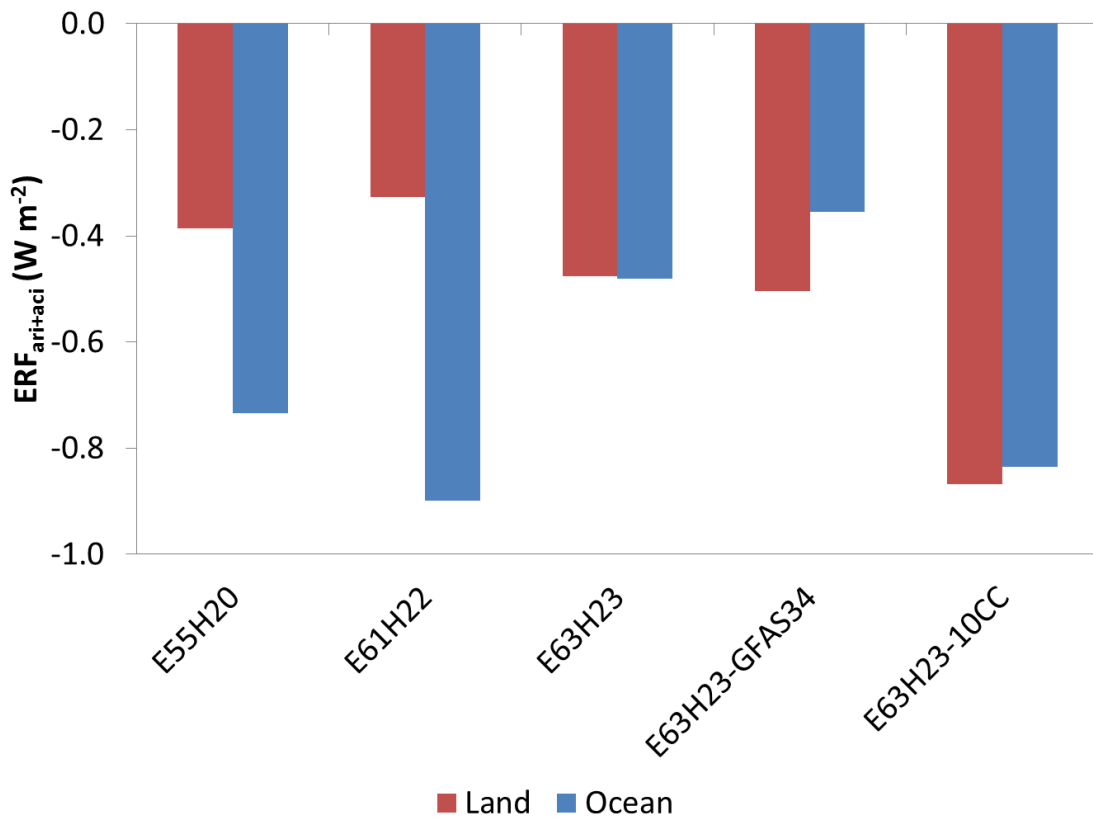
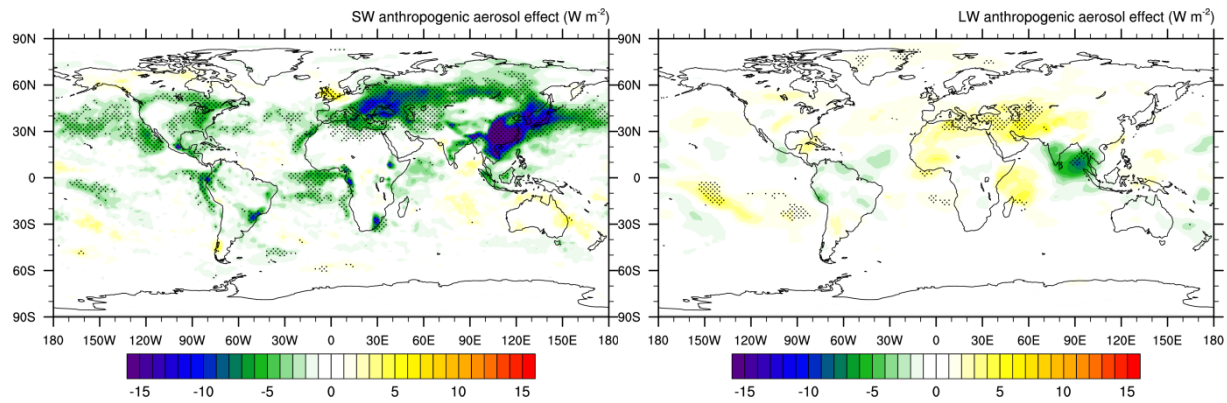
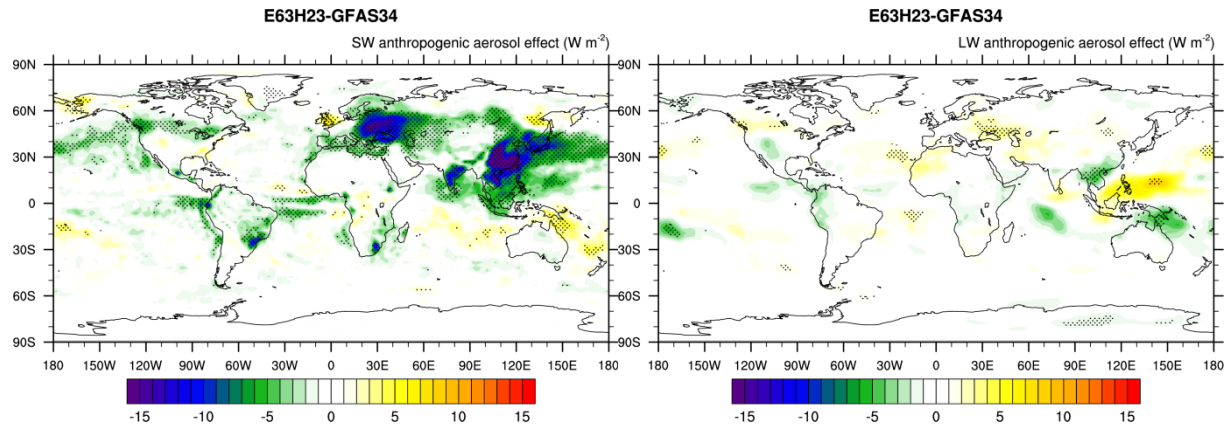
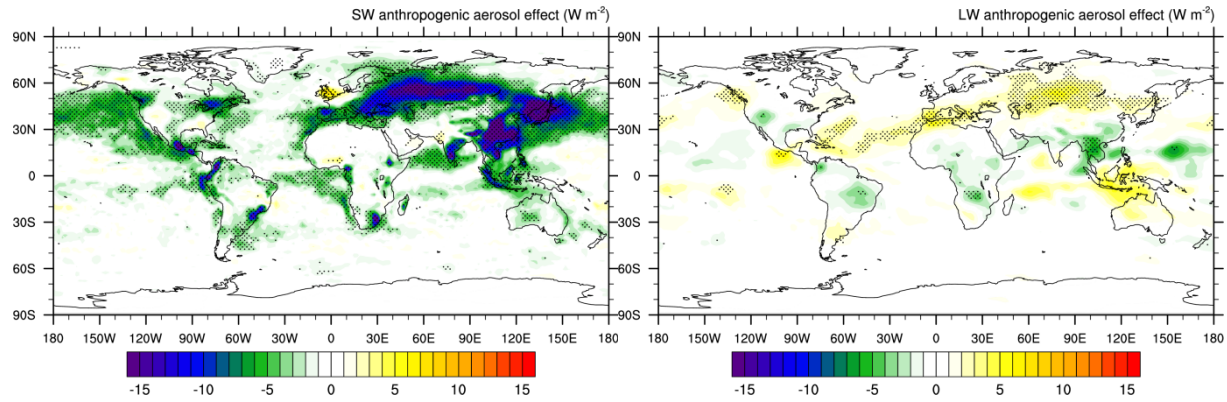
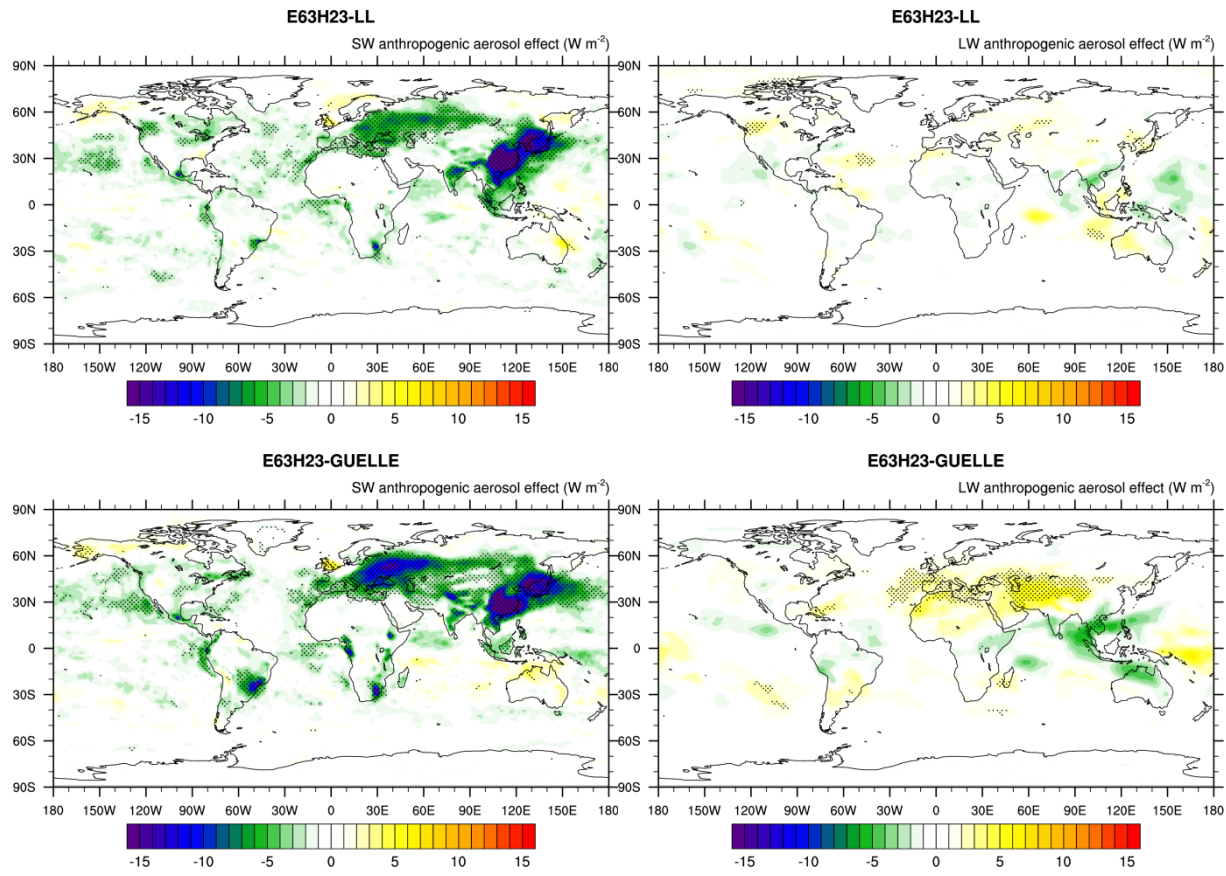


Figure S4: Global mean ERF_{ari+aci} over ocean and over land of E55H20, E61H22, E63H23, E63H23-GFAS34 and E63H23-10CC.

E63H23**E63H23****E63H23-CC10**

5



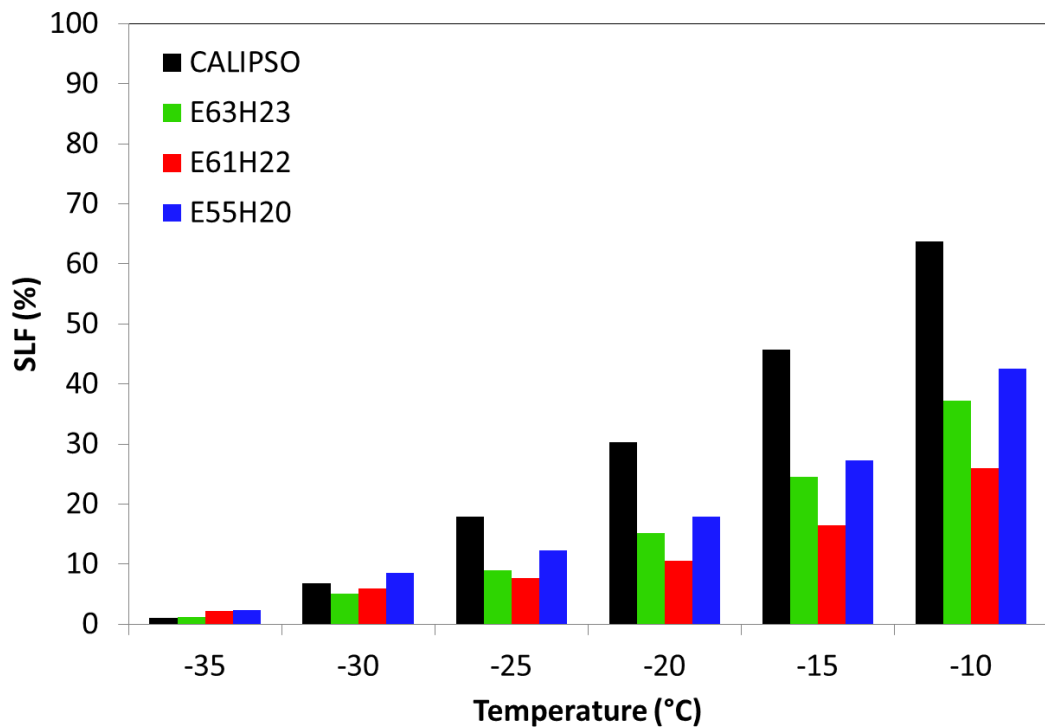
5 **Figure S5:** Global maps of SW and LW $\text{ERF}_{\text{ari+aci}}$ of E63H23, E63H23-GFAS34, E63H23-10CC, E63H23-LL and E63H23-GUELLE from 20 year free simulations with present day minus pre-industrial aerosol emissions ($\text{PD}_{\text{aer}} - \text{PI}_{\text{aer}}$). Hatching indicates statistically significant differences at the 95% significance level. The false discovery rate is controlled following Wilks (2016).

4 Global mean values of PD_{aer} , PI_{aer} , 1xCO₂ and 2xCO₂ simulations

Table S2. Global mean values of the PD_{aer}/PI_{aer} and 1xCO₂/2xCO₂ simulations for E55H20, E61H22 and E63H23. Radiative fluxes are at the top of atmosphere.

Variable	E55H20				E61H22				E63H23			
	PD _{aer} (20 years)	PI _{aer} (20 years)	2xCO ₂	1xCO ₂	PD _{aer} (20 years)	PI _{aer} (20 years)	2xCO ₂	1xCO ₂	PD _{aer} (20 years)	PI _{aer} (20 years)	2xCO ₂	1xCO ₂
SW (W m ⁻²)	232	233	237	232	236	238	241	237	238	240	242	239
LW (W m ⁻²)	-232	-232	-237	-233	-236	-236	-240	-237	-238	-238	-241	-239
Net(W m ⁻²)	-0.1	1.0	0.0	-0.4	0.4	1.6	0.4	0.1	0.5	1.5	0.5	0.2
SW CRE (W m ⁻²)	-53	-52	-50	-53	-52	-50	-49	-51	-50	-49	-48	-49
LW CRE (W m ⁻²)	28	28	26	29	27	26	25	27	24	24	23	25
Net CRE (W m ⁻²)	-25	-24	-24	-25	-24	-24	-24	-24	-26	-25	-25	-25
CC (%)	64	63	61	63	64	63	61	63	69	68	66	68
LWP (ocean) (g m ⁻²)	85	80	80	79	94	88	90	88	71	68	71	67
IWP (g m ⁻²)	8	8	8	9	10	10	10	10	15	15	14	15
Surface temperature (K)	288.8	288.8	291.6	288.1	289.0	289.0	291.3	288.5	288.8	288.9	291.1	288.6
CDNC _{burden} (10 ¹⁰ m ⁻²)	3.1	2.4	2.3	2.4	3.2	2.6	2.7	2.6	3.1	2.5	2.5	2.5
ICNC _{burden} (10 ¹² m ⁻²)	9.0	7.6	6.4	8.1	17.8	14.9	13.3	15.4	8.0	7.9	7.0	8.2
P (mm d ⁻¹)	3.0	3.0	3.2	3.0	3.0	3.0	3.2	3.0	3.0	3.0	3.1	3.0
Sulfate burden (Tg)	2.5	1.3	1.4	1.3	1.8	0.8	0.8	0.8	2.2	1.2	1.2	1.2
Black carbon burden (Tg)	0.13	0.03	0.03	0.14	0.08	0.08	0.08	0.08	0.14	0.08	0.08	0.08
Particulate organic matter burden (Tg)	1.1	0.5	0.5	1.1	0.9	1.0	0.9	1.0	0.8	0.9	0.8	0.8
Sea salt burden (Tg)	12.6	12.7	12.8	12.2	10.9	10.9	11.3	10.9	4.1	4.1	4.6	4.0
Mineral dust burden (Tg)	8.0	8.2	8.3	7.0	11.3	13.0	15.0	12.3	18.4	22.7	21.3	20.8

5 Supercooled liquid fraction (SLF)



5

Figure S6: Global mean of SLF (=liquid water content/(liquid water content+IWC)) for clouds with COD < 3 in different temperature bins for E55H20, E61H22 and E63H23. CALIPSO data is for the years 2006-2010 and the model data is from the PD simulations.

6 Zonal mean CDNC

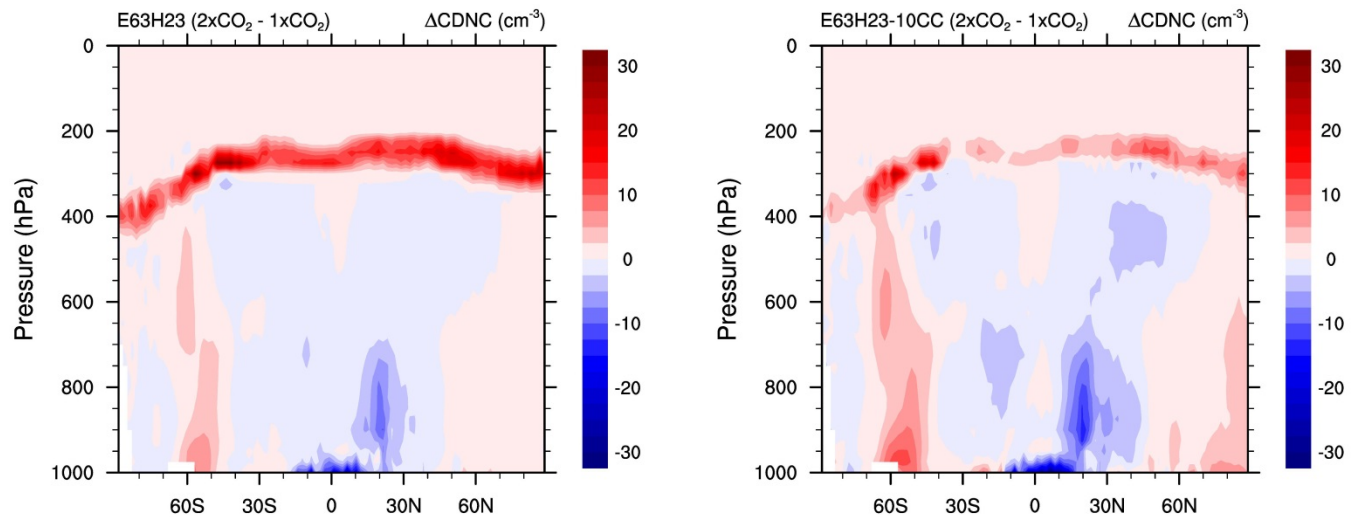


Figure S7: Zonal mean change in in-cloud CDNC for E63H23 and E63H23-10CC for the change from the 1xCO₂ climate to the 2xCO₂ climate. Averages for the last 25 years of the 1xCO₂ and 2xCO₂ experiments were used to create the figure.

7 COSP Calipso simulator cloud cover

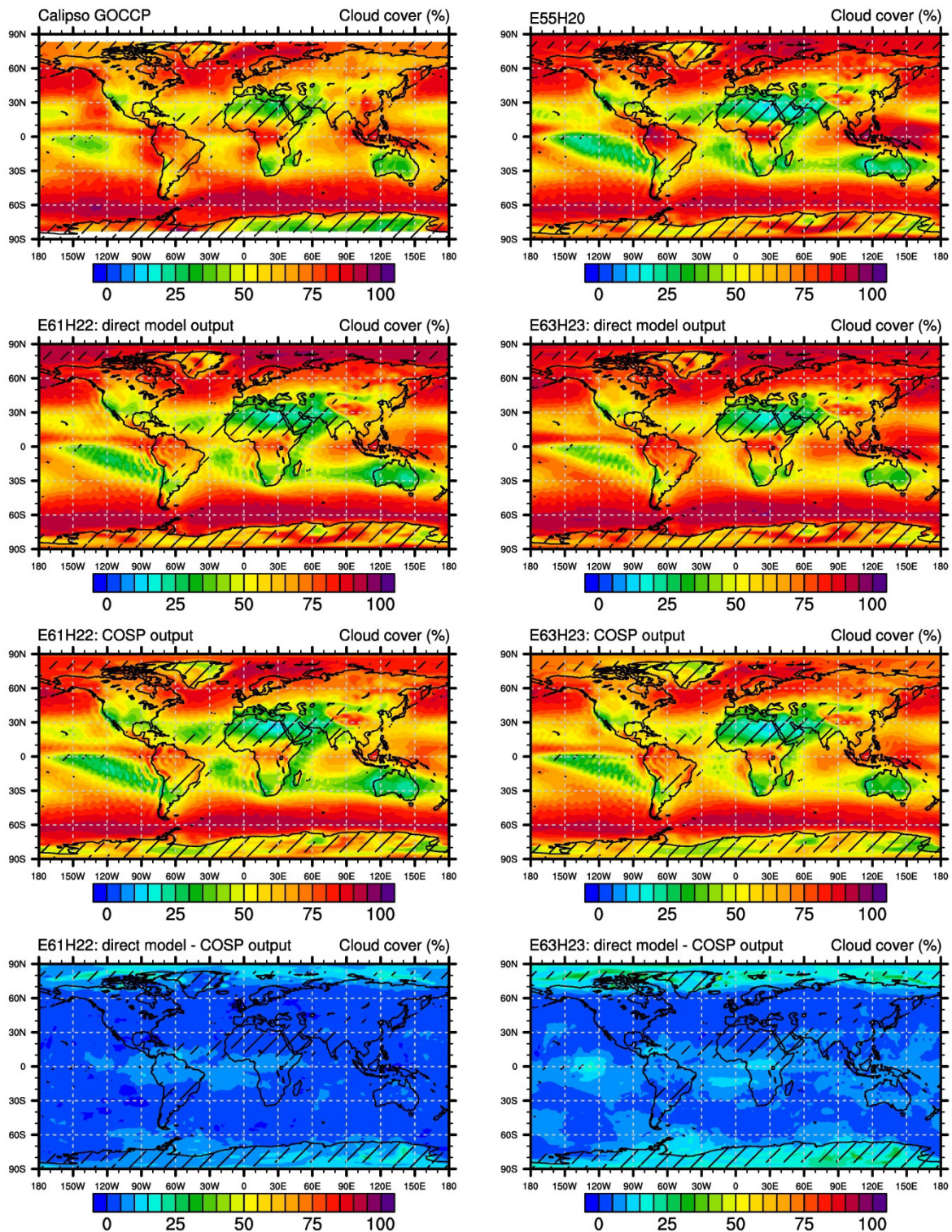


Figure S8: Comparison of annual mean cloud cover of E55H20, E61H22 and E63H23 to CALIPSO GOCCP observations. Areas where the cloud cover of CALIPSO GOCCP, MODIS collection 6.1 and AVHRR-PM differ by more than five percent points are hatched. CALIPSO GOCCP data is for 2006-2010, model data is from the PD simulations. For E61H22 and E63H23 the direct model output, the output of the COSP CALIPSO simulator implemented in those model versions and the difference between direct model output and COSP CALIPSO simulator output is displayed.

5